ELSEVIER

www.elsevier.nl/locate/ica

Inorganica Chimica Acta 313 (2001) 21–29

Inorganica Chimica Acta

Arylazoimidazoleplatinum(II) complexes and their dioxolene derivatives: single crystal X-ray structure of (catecholato){1-ethyl-2-(*p*-tolylazo)-imidazole}platinum(II)

S. Pal [a], D. Das [a], C. Sinha [a,*], C.H.L. Kennard [b]

[a] *Department of Chemistry, The University of Burdwan, Burdwan 713 104, India*
[b] *Department of Chemistry, The University of Queensland, St. Lucia, QLD 4072, Australia*

Received 11 May 2000; accepted 6 September 2000

Abstract

The reaction of 1-ethyl-2-(arylazo)imidazoles (RaaiEt, **1**) [R = H (**1a**), *p*-Me (**1b**), *p*-Cl (**1c**)] with K_2PtCl_4 in boiling acetonitrile–water (1:1) produces red–brown Pt(RaaiEt)Cl_2 (**2**) complexes. Addition of dioxolene in the presence of Et_3N to chloroform–methanol solution of Pt(RaaiEt)Cl_2 has yielded green-coloured mixed-ligand complexes [Pt(RaaiEt)(O,O)] [O,O = catecholate (cat) (**3**), 4-*tert*-butylcatecholate (tbcat) (**4**), 3,5-di-*tert*-butylcatecholate (dtbcat) (**5**), tetrachlorocatecholate (tccat) (**6**)]. The structure of [Pt(*p*-MeaaiEt)(cat)]·1/2H_2O (**3b**) was confirmed by X-ray diffraction. Electronic spectra exhibit ligand-to-ligand charge transfer transition (LLCT) in the VIS–NIR region; the position and symmetry of the band depend on the substituent type on the dioxolene and arylazoimidazole frames. This is qualitatively assigned as a HOMO(cat) → LUMO(RaaiEt) transition. Cyclic voltammograms of the complexes show four successive redox responses: two couples at positive to saturated calomel electrode (SCE) correspond to catechol to semiquinone and semiquinone to quinone oxidations, and two couples at negative to SCE correspond to the azo reductions. The difference in the potential $E_{1/2}$ of the first oxidation and reduction process changes linearly with the LLCT transition.

Keywords: Pt(II)-azoimidazole; Catecholato complexes; LLCT; X-ray crystal structures; Electrochemistry

1. Introduction

This work is part of a systematic investigation on transition metal complexes of azoimine function in general [1–28] and arylazoimidazoles [19–27] in particular. Azoimines are isoelectronic with the diimine system [1], and the scope of this function encompasses from the stabilisation of the low-valent metal redox state [1–7,19–28], metaloxo complexes [8,9], formation of organometallic compounds [18] to the metal mediated C–H bond activation of the pendant aryl group following the hydroxylation [13], thiolation [14–16] and amination [12] reactions. This is part of our continuing work on platinum metal chemistry [1–15,19–28]. Metallated azoimine fragments exhibit potent M → L charge transfer transitions [1–7], and a reducing ligand, like dioxolene, in ternary complexes of redox-innocent metal ions shows efficient ligand-to-ligand charge transfer (LLCT) transition [24,29]. This exhibits a negative solvatochromic effect in palladium(II) complexes [29].

Platinum(II)–diimine complexes are important because of their charge transfer, luminescence, and electrochemical properties [30–32] and their catalytic [33], and biological [34–37] activities. The current research in the field of platinum(II) chemistry with N-donor ligands is aimed at synthesising compounds analogous to cisplatin [34–37]. Platinum(II)–catecholates have anti-cancer activity and are used to label the metalloantigens [38]. Platinum(II)–diimine–catecholato complexes exhibit solvent-dependent LLCT transitions [39]. This is a report of the synthesis, spectral characterisation and electrochemical properties of 1-ethyl-2-(arylazo)imidazole complexes of platinum(II) and their dioxolene derivatives. The structure of (catecholato){1-ethyl-2-(phenylazo)imidazole}platinum(II) is supported by X-ray crystallography.

* Corresponding author. Fax: +91-342 564452.
E-mail address: c_r_sinha@yahoo.com (C. Sinha).

0020-1693/01/$ - see front matter
PII: S0020-1693(00)00311-X

2. Experimental

2.1. Materials

$H_2PtCl_6 \cdot xH_2O$ was purchased from Arrora Matthey, Calcutta, India. K_2PtCl_4 was prepared from the reported method [40]. 1-Ethyl-2-(arylazo)imidazoles were synthesised according to the published procedure [21]. Pyrocatechol (H_2cat), 3,5-di-*tert*-butylcatechol (H_2dtbcat), and tetrachlorocatechol (H_2tccat) were obtained from Aldrich. 4-*tert*-Butylcatechol (H_2tbcat) was purchased from Fluka. Catechols were purified before use by recrystallisation from benzene. Dichloromethane and acetonitrile were further purified by distillation over P_4O_{10}. Bu_4NClO_4 was prepared according to the reported method [19]. Nitrogen was purified by bubbling through alkaline pyrogallol solution and concentrated H_2SO_4. Silica gel (60–120 mesh) for column chromatography was obtained from SRL. Triethylamine and other chemicals and solvents used for the preparative work were of reagent grade and were used as received.

2.2. Physical measurements

The IR spectra (KBr disk, 4000–200 cm^{-1}) were recorded on FTIR JASCO model 420. UV–VIS–NIR spectra were collected from Shimadzu UV 160A and Hitachi U-3501-UV–VIS–NIR spectrophotometers. ^1H NMR spectra were recorded on Brucker AC(F) 200 and 300 MHz FT-NMR spectrometers. Electrochemical studies were performed on a computer-controlled EG&G PAR model 270 VERSASTAT electrochemical instrument with Pt-disk and glassy carbon (GC) electrodes. All measurements were carried out under dinitrogen environment at 298 K with reference to a saturated calomel electrode (SCE) in acetonitrile. $[Bu_4N][ClO_4]$ was used as the supporting electrolyte. The reported potentials are uncorrected for junction potential. Microanalytical data were obtained from a Perkin Elmer 2400 CHNS/O elemental analyser.

2.3. Preparation of dicholoro-{1-ethyl-2-(phenylazo)imidazole}platinum(II), Pt(HaaiEt)Cl_2, (**2a**)

1-Ethyl-2-(phenylazo)imidazole (HaaiEt) (0.42 g, 2.10 mmol) in MeCN–water (15 cm^3) was added dropwise to an MeCN–water (1:1, v/v; 40 cm^3) solution of K_2PtCl_4 (0.85 g, 2.05 mmol) and the mixture was refluxed for 48 h. On slow evaporation, a brown precipitate gradually appeared; this was filtered and washed with cold MeCN–water (1:1, v/v, 3 × 5 cm^3). The dried mass was dissolved in a minimum volume of CH_2Cl_2 and chromatographed over a silica gel column. The desired compound was eluted as a brown–red band by C_6H_6–MeCN (2:1, v/v); yield, 0.48 g (50%). Other complexes were prepared under identical conditions, and yields varied in the range 45–50%.

2.4. Preparation of catecholato{1-ethyl-2-(phenylazo)imidazole}platinum(II), [Pt(HaaiEt)(cat)], (**3a**)

Pyrocatechol (0.098 g, 0.89 mmol) in MeOH (10 cm^3) was added to Pt(HaaiEt)Cl_2, **2a**, (0.395 g, 0.85 mmol) which had been dissolved in degassed $CHCl_3$–MeOH mixture (50% v/v, 30 cm^3). Triethylamine (2 mmol) under N_2 was added to this solution, stirred for 1 h and the colour changed from brown–red to green. N_2 bubbling through the solution evaporated it to a third of its original volume, producing a dark green precipitate that was filtered, washed with cold MeOH and dried in vacuo. The dried mass was dissolved in a minimum volume of CH_2Cl_2 and chromatographed over a silica gel column to give the desired green band, which was eluted with a 3:2 (v/v) C_6H_6–MeCN mixture. On evaporation a crystalline product was produced with a yield of 0.208 g (41%). All other complexes were prepared by similar procedures, with yields varying in the range 40–55%.

2.5. X-ray crystal structure determination

Crystals suitable for X-ray work were grown by slow diffusion of benzene into CH_2Cl_2 solution of the complex [Pt(*p*-MeaaiEt)(cat)]·1/2H_2O (**3b**). Crystal size is 0.11 × 0.10 × 0.15 mm^3. Data were collected from an Enraf–Nonius CAD 4 four-cycle diffractometer employing graphite monochromatised Mo Kα radiation ($\lambda = 0.710\ 69$ Å) at 293 K. Crystal data and data collection parameters are listed in Table 1. The data are corrected for absorption (Ψ scans) using the XTAL package [41–43]. The compound crystallised in $P\bar{1}$. Of the 6660 reflections collected, 6220 with $I > 2\sigma(I)$ (CHECK) were used for structure solution. The structure was solved using the heavy atom-Patterson method with SHELXS86 and refined by full-matrix least-squares analysis with SHELXL97. All non-hydrogen atoms were refined using anisotropic thermal parameters, and H-atoms located from difference maps and refined isotropically.

3. Results and discussion

3.1. Synthesis

Reaction of K_2PtCl_4 with 1-ethyl-2-(arylazo)-imidazoles (RaaiEt, **1**) in acetonitrile–water mixture under reflux produced red–brown Pt(RaaiEt)Cl_2

Table 1
Crystallographic data and structure refinement for [Pt(*p*-MeaaiEt)(cat)] (**3b**)

Empirical formula	$C_{18}H_{18}N_4O_{2.5}Pt$
Formula weight	525.45
Temperature (K)	293(2)
Wavelength (nm)	0.710 69
Crystal system	Triclinic
Space group	$P\bar{1}$
a (Å)	8.8479(11)
b (Å)	11.3939(11)
c (Å)	17.802(2)
α (°)	89.950(9)
β (°)	83.669(10)
γ (°)	82.462(9)
Volume (Å^3)	1768.1(4)
Z	4
ρ_{calc} (g cm^{-3})	1.974
μ (mm^{-1})	7.959
$F(000)$	1008
Crystal size (mm^3)	$0.11 \times 0.10 \times 0.75$
2θ (°)	$4 \leq 2\theta \leq 50$
Index ranges	$0 \leq h \leq 10$, $-13 \leq k \leq 13$, $-21 \leq l \leq 21$
Reflections collected	6660
Independent reflections	6220 ($R_{int} = 0.0430$)
Data/restraints/parameters	6220/0/460
Goodness-of-fit on F^2	0.981
Final R indices [$I > 2\sigma(I)$]	$R_1 = 0.0563$, $wR_2 = 0.0970$
R indices (all data)	$R_1 = 0.0563$, $wR_2 = 0.1050$
Largest diff. peak and hole (e$^-$ A^{-3})	2.272 and −1.652

(**2**). The addition of Et_3N to the solution of **2** and catechol in a $CHCl_3$–MeOH mixture under N_2 changes the colour immediately from brown–red to green and the product separates on slow bubbling of N_2 for a period of 1 h or more (Scheme 1). Solvent removal followed by the chromatographic purification gave green catecholato complexes [Pt(RaaiEt)(O,O)]. The catechols used are abbreviated as pyrocatechol (H_2cat), 4-*tert*-butyl catechol (H_2tbcat), 3,5-di-*tert*-butyl catechol (H_2dtbcat), tetrachlorocatechol (H_2tccat) and have the complexes Pt(RaaiEt)(cat) (**3**), Pt(RaaiEt)(tbcat) (**4**), Pt(RaaiEt)(dtbcat) (**5**) and Pt(RaaiEt)(tccat) (**6**). The complexes are non-conducting and the elemental analyses (Table 2) support the composition of the complexes.

3.2. Single crystal X-ray structure of [Pt(p-MeaaiEt)(cat)] (3b)

The complex [Pt(*p*-MeaaiEt)(cat)] crystallises in $P\bar{1}$ with two molecules in the asymmetric unit (Fig. 1), which are different as the ethyl group about N41 has a different conformation. The water molecule O(1W) is hydrogen bonded to O(5B). No hydrogen atoms were found for this molecule, although the oxygen has relatively short links at 2.7 Å to H(43A) and H(43B). The selected bond parameters are listed in Table 3. The PtN_2O_2 is a square plane (deviation < 0.04 Å). Two chelate planes Pt, N(1), N(4) (mean deviation 0.02 Å) and Pt, O(5), O(6) (mean deviation 0.03 Å) are planar. The chelate angles N(1)–Pt–N(4) and O(5)–Pt–O(6) are 79.0(3)° (A), 77.8(3)° (B) and 83.4(2)° (A), 82.6(2)° (B) respectively for molecules A and B (given in the parentheses). Two chelate planes are inclined at an angle 5.84° (A), 5.02° (B). The pendant *p*-tolyl ring is planar and is inclined at an acute angle 21.10° (A), 23.35° (B) with the N(1)–Pt–N(4) chelate ring. This magnetically distinguishes two ortho C–H functions [19] and is seen in the ^{1}H NMR spectra (vide infra). The average

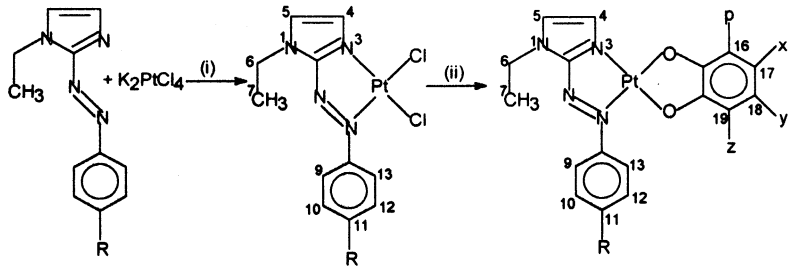

R = H (1a), CH_3 (1b), Cl (1c)

	3	4	5	6
p	H	H	Bu^t	Cl
x	H	Bu^t	H	Cl
y	H	H	Bu^t	Cl
z	H	H	H	Cl

Scheme 1. (i) MeCN–water (1:1), reflux, 48 h. (ii) Catechols, Et_3N in $CHCl_3$–MeOH, stirred, under N_2 atmosphere.

Table 2
Microanalytical, UV–VIS and electrochemical data

Compound	Elemental analyses: found (calc.) (%)			UV–VIS λ_{max} (nm) [ε ($dm^3\ mol^{-1}\ cm^{-1}$)]	Cyclic voltammetry[a]				
	C	H	N		Rcq/Rsq $E^1_{1/2}$ (V) [ΔE_p (mV)[d]]	Rsq/q $E^2_{1/2}$ (V) [ΔE_p (mV)[d]]	azo$^-$/azo $-E^3_{1/2}$ (V) [ΔE_p (mV)[d]]	$\Delta E_{1/2}$ (V)[e]	$\bar{\nu}_{CT}$[f] (eV)
Pt(HaaiEt)Cl_2	28.40 (28.32)	2.52 (2.57)	12.00 (12.01)	545[b] [165], 482 [457], 412 [14 410]			0.404 [70]		
Pt(MeaaiEt)Cl_2	30.15 (30.00)	2.86 (2.92)	11.58 (11.66)	541[c] [167], 482 [424], 417 [14 757]			0.470 [75]		
Pt(ClaaiEt)Cl_2	26.40 (26.37)	2.24 (2.20)	11.13 (11.18)	553 [160], 484 [424], 415 [14 240]			0.349 [70]		
Pt(HaaiEt)(cat)	40.50 (40.55)	3.10 (3.18)	11.18 (11.13)	807 [7050], 630 [3292], 403 [13 251]	0.414 [105]	0.850[c]	0.842 [120]	1.256	1.538
Pt(HaaiEt)(tbcat)	45.10 (45.08)	4.30 (4.29)	9.85 (10.01)	841 [5356], 634 [2639], 405 [9773]	0.353 [80]	0.686 [120]	0.871 [120]	1.221	1.476
Pt(HaaiEt)(dtbcat)	48.70 (48.78)	5.00 (5.20)	8.50 (9.10)	925 [6074], 654 [2230], 468 [3844][c]	0.247 [85]	0.524 [100]	0.884 [130]	1.131	1.342
Pt(HaaiEt)(tccat)	31.75 (31.82)	1.80 (1.87)	8.75 (8.73)	725 [7950], 600 [4776], 408 [16 348]	0.780[c]		0.743 [90]		
Pt(MeaaiEt)(cat)	41.85 (41.77)	3.50 (3.48)	10.73 (10.83)	790 [7782], 619 [3393], 415 [14 886]	0.400 [104]	0.810[c]	0.878 [130]	1.278	1.571
Pt(MeaaiEt)-(tbcat)	46.00 (46.07)	4.50 (4.53)	9.80 (9.77)	822 [2215], 628 [1887], 420 [8191]	0.338 [100]	0.660 [120]	0.924 [160]	1.262	1.510
Pt(MeaaiEt)-(dtbcat)	49.56 (49.60)	5.34 (5.40)	8.15 (8.90)	888 [3467], 659 [1739], 417 [9622]	0.214 [90]	0.511 [150]	0.895 [140]	1.109	1.400
Pt(MeaaiEt)-(tccat)	32.90 (32.97)	2.10 (2.13)	8.50 (8.55)	723 [2830], 590 [2040], 420 [9350]	0.710[c]		0.791 [110]		
Pt(ClaaiEt)(cat)	37.90 (37.95)	2.75 (2.79)	10.35 (10.41)	841 [11 290], 634 [4806], 414 [21 504]	0.452 [94]	0.780[c]	0.753 [140]	1.205	1.476
Pt(ClaaiEt)-(tbcat)	42.40 (42.45)	3.80 (3.87)	9.45 (9.43)	883 [5179], 651 [2152], 412 [10 321]	0.381 [100]	0.630 [110]	0.764 [109]	1.154	1.405
Pt(ClaaiEt)-(dtbcat)	46.00 (46.18)	4.69 (4.77)	8.58 (8.62)	960 [6553], 667 [1831], 474 [4101], 407 [9533]	0.265 [120]	0.570 [100]	0.798 [180]	1.063	1.293
Pt(ClaaiEt)(tccat)	30.00 (30.19)	1.60 (1.62)	8.00 (8.29)	741 [625], 590 [476], 412 [1723]	0.830[c]		0.665 [140]		

[a] Solvent is dichloromethane.
[b] Shoulder.
[c] E_{pa} (V).
[d] $\Delta E_p = E_{pa} - E_{pc}$ (mV).
[e] $\Delta E_{1/2} = E^1_{1/2} - E^3_{1/2}$ (V).
[f] $\nu_{CT} = 1241/\lambda_{max}$ (nm).

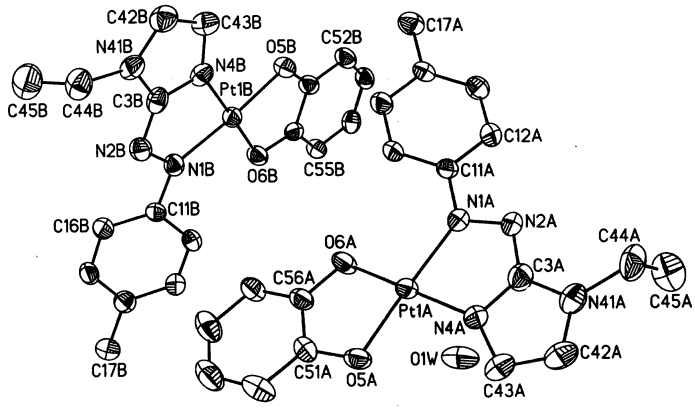

Fig. 1. Single crystal structure of [Pt(ρ-MeaaiEt)(cat)]. For clarity, all hydrogen atoms have been eliminated.

Pt–N(azo) (Pt–N(1)) and Pt–N(imidazole) (Pt–N(4)) distances are approximately 1.980(6) (A), 1.971(6) Å (B) and 1.980(6) (A), 1.974(6) Å (B) respectively. Although the two catecholato-O are equivalent [44], they are distinctly different in terms of the Pt–O and C–O bond distances in this complex. The Pt–O(6) is elongated by approximately 0.03 Å compared with Pt–O(5). The C–O(6) is shorter than C–O(5) by 0.04 Å, but is far away from the semiquinone bond length [45]. This observation is corroborated with the higher trans-influence provided by N(4) (N(imidazole)) than by N(1) (N(azo)). From available structural reports on platinum metal compounds of azoimine, the function M–N(azo) is shorter than the M–N(imine) distance (M = Ru [46], Os [3], Re [4], Pd [47], Pt [48]). The shortening may be due to the greater π back-bonding, represented as $M(d\pi) \rightarrow \pi^*$(azo). This also enhances the N=N bond length relative to the free ligand value (1.25 Å) [3,49]. The X-ray structure determination of dichloro-[1-ethyl-2-(naphthyl-β-azo)imidazole]platinum(II) suggests that the N=N length is 1.280(5) Å [50]. The present structure has the longest N=N bond (1.32 Å) in the platinum metal chemistry; this may be due to charge delocalisation from catechol to the azo function in the coordinated frame involving metal dπ-orbitals, which is supported from solution (VIS–NIR), magnetic (^{1}H NMR) and redox properties.

The Pt–N(1) and Pt–N(4) distances are comparable. This is quite unusual compared with similar bond lengths in other platinum metal complexes [3,4,46,47], and in the case of Pt(II)–naphthylazoimidazole [50] it follows the order Pt–N(4) (1.983(4) Å) < Pt–N(1) (2.039 Å). This may be due to the preferential binding of platinum(II) to imidazole-N than other N(sp^2) centres present in the same molecule. It is observed in the 1-methylimidazole-2-yl-pyridine-2-yl ketone Pt(II) complex that the Pt–N(imidazole) is shorter than the Pt–N(pyridine) distance [51]. Biological molecules and DNA bases also prefer to bind cisplatin via N(imidazole) (N(7) of guanine, adenine) [37].

3.3. Spectral characterisation

The IR spectrum of $Pt(RaaiEt)Cl_2$ (**2**) exhibits a single sharp stretch at approximately 1385–1395 cm^{-1} corresponding to ν(N=N) compared with free ligand values (approximately 1410 cm^{-1}). The *cis*-$PtCl_2$ configuration was established by the appearance of ν(Pt–Cl) at 350 and 335 cm^{-1} [13,52]. For catecholato complexes, [Pt(RaaiEt)(O,O)], the N=N stretch appears at approximately 1340 cm^{-1} and the lowering of the frequency may be attributed to the extensive $d(Pt) \rightarrow \pi^*$(RaaiEt) back bonding or $3b_1$(cat) $\rightarrow \pi^*$(RaaiEt) in the catecholato comlexes [29]. The appearance of a broad band at 3400 cm^{-1} supports the presence of H_2O in the molecule. On comparing the spectra of $Pt(RaaiEt)Cl_2$ and [Pt(RaaiEt)(O,O)], additional bands are observed at 1250–1280 and 1460–1470 cm^{-1} corresponding to C–O (phenolic) vibrations of catechols and at approximately 555 cm^{-1} for (Pt–O).

Table 3
Selected bond distances and angles and their estimated standard deviations for **3b**

Distances (Å)		Angles (°)	
Pt(1A)–N(1A)	1.980(6)	N(1A)–Pt(1A)–N(4A)	79.8(3)
Pt(1A)–N(4A)	1.980(6)	O(5A)–Pt(1A)–O(6A)	83.4(2)
Pt(1A)–O(5A)	1.956(6)	N(1A)–Pt(1A)–O(5A)	176.0(2)
Pt(1A)–O(6A)	1.994(5)	N(4A)–Pt(1A)–O(6A)	176.3(2)
Pt(1B)–N(1B)	1.971(6)	N(1A)–Pt(1A)–O(6A)	100.0(2)
Pt(1B)–N(4B)	1.974(6)	N(4A)–Pt(1A)–O(5A)	97.5(3)
Pt(1B)–O(5B)	1.949(5)	N(1B)–Pt(1B)–N(4B)	77.8(3)
Pt(1B)–O(6B)	1.978(5)	O(5B)–Pt(1B)–O(6B)	82.6(2)
N(1A)–N(2A)	1.320(9)	N(1B)–Pt(1B)–O(5B)	175.7(2)
N(1B)–N(2B)	1.319(9)	N(4B)–Pt(1B)–O(6B)	177.2(2)
C(51A)–O(5A)	1.376(10)	N(1B)–Pt(1B)–O(6B)	101.4(2)
C(56A)–O(6A)	1.327(9)	N(4B)–Pt(1B)–O(5B)	98.2(2)
C(51A)–C(56A)	1.388(11)		
C(51B)–O(5B)	1.361(9)		
C(56B)–O(6B)	1.333(9)		
C(51B)–C(56B)	1.385(11)		

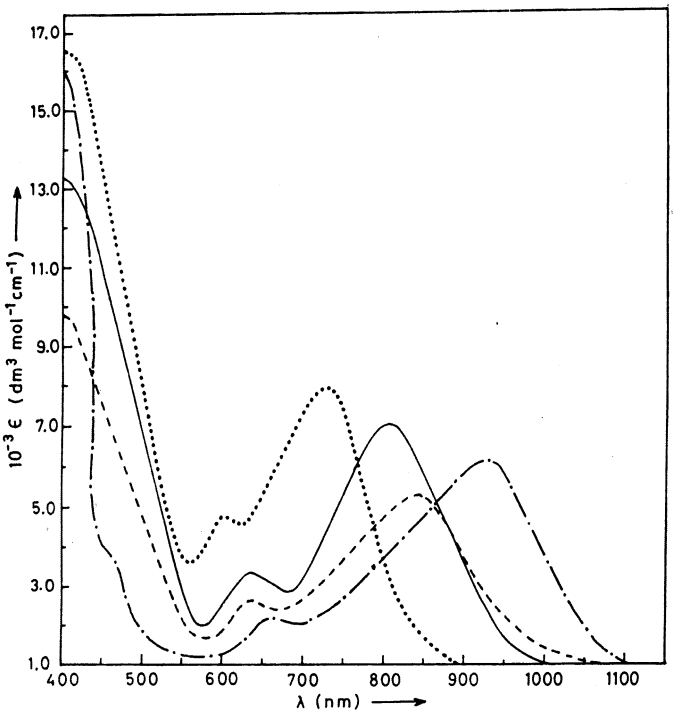

Fig. 2. Electronic absorption spectra of [Pt(HaaiEt)(cat)] (—); [Pt(HaaiEt)(tbcat)] (- - -); and [Pt(HaaiEt)(dtbcat)] (— · —); and [Pt(HaaiEt) (tccat)] (· · ·) in CH_2Cl_2 at 298 K.

The electronic spectra of the complexes were examined in chloroform. Pt(RaaiEt)Cl_2 exhibits three absorption bands in the visible region at 415, 480 and 545 nm. The transitions below 400 nm are due to an intraligand charge transfer transition [21] and are not considered further. The absorption spectra of catecholato complexes [Pt(RaaiEt)(O,O)] are different than Pt(RaaiEt)Cl_2 (Fig. 2, Table 2). A new band appears in the red to NIR region and is dependent on the nature of the substituent in dioxolene and azoimidazole fragments [24,29,39]. This band has been assigned as an LLCT transition involving the HOMO of catechol and the LUMO of RaaiEt [53] or the redox orbital constituted by platinum(II) and ligand [39]. The electron-donating substituent (–Me group) in the MeaaiEt site moves the band position to the shorter wavelength region and the reverse is true for the electron-withdrawing substituent (–Cl group) in ClaaiEt. Thus the wavelength order follows MeaaiEt < HaaiEt < ClaaiEt. The wavelength trend of the absorption band for a particular RaaiEt in [Pt(RaaiEt)(O,O)] is tccat < cat < tbcat < dtbcat. The HOMO of dtbcat is expected to have the highest energy in the series because of the electron-releasing effect of two ^{t}Bu groups. In tccat, the HOMO has the lowest energy in the series because of the electron-withdrawing character of the –Cl groups. The LUMO is characterised by an azoimidazole function; in ClaaiEt the energy of the π*(LUMO) is of lower value than HaaiEt because of the electron-withdrawing effect of the Cl group, and the reverse is true for MeaaiEt because of the + I effect of the –Me group.

The proton numbering scheme for ^{1}H NMR spectra is shown for structures **2**–**6** with data summarised in Table 4. All aromatic protons of the complexes were assigned on the basis of spin–spin interactions and changes on substitution. The N–Et signal in Pt(RaaiEt)Cl_2 is supported by the appearance of a triplet and a quartet signal at approximately 1.6 ppm and 4.5 ppm respectively. Imidazole 4- and 5-H appear at 7.6 ppm and 7.4 ppm respectively and are downfield shifted by > 0.4 ppm compared with the free ligand values. This is in support of strong Pt(II) bonding with the imidazole group. The aryl protons are also downfield shifted with reference to the free ligand values and are moved to higher and lower δ values in the usual manner with the substituents [49]. In catecholato complexes the RaaiEt protons, in general, suffer significant upfield shifting by 0.2–1.0 ppm compared with the parent chloro complex, with the exception of a doublet signal of a proton (as evident from integration). The signal shifting to an upfield position is due to the charge being delocalised from the HOMO (cat) to the LUMO (RaaiEt) [29]. The appearance of a downfield doublet could be due to the asymmetric orientation of the pendant aryl ring in the ligand. This magnetically differentiates between the 9- and 13-H, where 9-H is considered stereochemically nearer to the metal centre. The X-ray structural data also support this inference; the *p*-tolyl plane is inclined at acute angle (21.1°) to the corresponding chelate plane (vide supra). The coordination of imidazole-N to Pt(II) is again supported by coupling of 4-H with ^{195}Pt ($I = 1/2$, abundance 33.7%) and the coupling constant ^3J(Pt–H) is 20–25 Hz [54]. The protons of the catecholato ring are on the upfield side relative to the RaaiEt; this is caused by the electron-releasing effect of the catecholato oxygen. The complexes [Pt(RaaiEt)(cat)] give a characteristic AA′BB′ pattern, whereas signals in the aliphatic region (δ, 1.2, 1.4 ppm) are due to the ^{t}Bu group in Pt(RaaiEt)(tbcat)/Pt(RaaiEt)(dtbcat) complexes. Other protons in the dioxolene ring are easily identified by comparing the results reported elsewhere [29].

3.4. Electrochemical studies

The complexes exhibit three/four successive cyclic redox systems within the potential range + 1.5 to − 1.5 V versus SCE. The electrochemical measurements were carried out with the use of a Pt working electrode for Pt(RaaiEt)Cl_2 (**2**) and a GC working electrode for [Pt(RaaiEt(O,O)] (**3**, **6**) in acetonitrile solution under dinitrogen in the presence of tetrabutylammonium perchlorate (Bu_4NClO_4) as a supporting electrolyte. The couples appearing at the negative side to the SCE correspond to azo reduction. The LUMO of azo can

accommodate two electrons and, hence, two reductions are observed (Eq. (1)).

$$[\text{–N=N–}] \overset{+e^-}{\rightleftharpoons} [\text{–N}\cdots\text{N–}]^{-} \overset{+e^-}{\rightarrow} [\text{–N–N–}]^{2-} \quad (1)$$

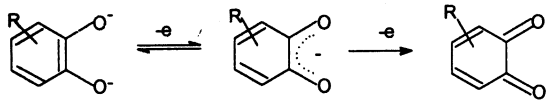

(2)

The anodic responses are due to coordinated catechol oxidation (Eq. (2)) with the compounds undergoing two successive one-electron redox responses with varying degrees of reversibility depending upon the substituent in the catechol ring [29,55].

The complexes [Pt(RaaiEt)(tbcat)] and [Pt(RaaiEt)-(dtbcat)] give reversible first oxidation couples (ΔE_p = 70–90 mV) followed by a quasi-reversible response ($\Delta E_p > 120$ mV), as evident from peak-to-peak separation. The data in Table 1 reveal that E_{pa} (anodic peak potential) is shifted to more positive values due to the presence of the electron-withdrawing –Cl group in Pt(RaaiEt)(tccat) and the reverse is observed for butyl groups (Fig. 3). This is because oxidation will be thermodynamically more facile when electron density flows into the catechol ring, leading to the stabilisation of the positive charge of the cation radical [56]. Thus, reduction refers to the electron accommodation at the LUMO (azo characterised) and oxidation is the electron extraction from the HOMO (catechol characterised). The difference in potential between the first reduction and first oxidation ($\Delta E_{1/2} = E^1_{1/2} - E^3_{1/2}$) may be correlated with the LLCT (ν_{CT}) transitions that are observed in the low-energy region (Eq. (3)). This supports the involvement of the same redox orbitals in charge transfer transition and redox reactions.

$$\nu_{CT} = 1.174\Delta E_{1/2} + 0.052 \quad (3)$$

3.5. Comparison with analogous palladium complexes

Table 5 summarises some spectral and electrochemical data of the palladium(II) [24,49] and platinum(II) complexes of analogous 1-ethyl-arylazoimidazoles. It shows that the LLCT band position is shifted to a shorter wavelength region, $E_{1/2}$ of dioxolenes is moved to less positive values and $-E_{1/2}$ of azo is also transferred to more negative values on traversing from palladium(II) to platinum(II). The spectral trend accounts for the larger energy difference between the participating HOMO and LUMO in platinum(II) complexes and is more destabilised relative to palladium(II) complexes. This may be due to the participation of metal-redox orbitals with ligand-group of orbitals more efficiently in platinum than palladium complexes. This is a general group trend in the family of platinum metals and the 5d-orbitals are relativistically more perturbed by the external field than 4d-orbitals [57]. This observation is

Table 4
^{1}H NMR spectral data in $CDCl_3$

Compound[a]	δ (ppm)											
	4-H[b,e]	5-H[b]	9-H[b]	10,12-H	13-H[b]	6-CH_2–	7–CH_3[c]	16-H	17-H	18-H	19-H	Others
Pt(HaaiEt)Cl_2	7.40	7.24	8.00	7.71[c]	8.00	4.55	1.62					
Pt(MeaaiEt)Cl_2	7.37	7.22	7.95	7.62[b]	7.95	4.52	1.60					2.43[g]
Pt(ClaaiEt)Cl_2	7.49	7.29	8.16	7.85[b]	8.16	4.58	1.62					
Pt(HaaiEt)(cat)	7.18	7.04	8.22	7.50[c]	7.80	4.25	1.58	7.04[b]	6.51[d]	6.51[d]	7.04[b]	
Pt(HaaiEt)(tbcat)	7.10	6.97	8.16	7.46[c]	7.74	4.24	1.54	6.78[f]		6.58[b]	6.89[b]	1.30[h]
Pt(HaaiEt)(dtbcat)	7.03	6.81	8.12	7.44[c]	7.66	4.19	1.50		6.63[f]		6.40[g]	1.33[h], 1.27[h]
Pt(HaaiEt)(tccat)	7.20	7.07	8.25	7.55[c]	7.93	4.43	1.58					
Pt(MeaaiEt)(cat)	7.20	7.05	8.25	7.35[b]	7.85	4.28	1.55	6.52	7.01[d]	7.01[d]	6.52	2.41[h]
Pt(MeaaiEt)(tbcat)	7.15	7.00	8.22	7.33[b]	7.78	4.25	1.54	6.67[f]		6.44[b]	6.69[b]	2.40[h], 1.30[h]
Pt(MeaaiEt)(dtbcat)	7.11	6.94	8.20	7.30[b]	7.84	4.24	1.50		6.58[f]		6.39[g]	2.40[g], 1.33[h], 1.26[i]
Pt(MeaaiEt)(tccat)	7.24	7.10	8.28	7.42[b]	7.94	4.33	1.55					2.42[g]
Pt(ClaaiEt)(cat)	7.16	7.03	8.30	7.44[b]	8.00	4.20	1.55	6.53[b]	6.97[d]	6.97[d]	6.53[b]	
Pt(ClaaiEt)(tbcat)	7.11	6.93	8.28	7.42[b]	7.96	4.35	1.55	6.69[f]		6.48[b]	6.82[b]	1.28[h]
Pt(ClaaiEt)(dtbcat)	7.00	6.60	8.25	7.38[b]	7.90	4.30	1.22		6.84[f]		6.68[g]	1.27[h], 1.41[h]
Pt(ClaaiEt)(tccat)	7.25	7.09	8.40	7.68[b]	8.14	4.40	1.30					

[a] With Me_4Si as internal standard.
[b] Doublet (J = 7.0–8.0 Hz).
[c] Triplet (J = 10.0–11.0 Hz).
[d] Multiplet (J = 7.0–8.0 Hz).
[e] $^3J_{Pt-H}$ = 20–25 Hz.
[f] Singlet.
[g] p-Me.
[h] ^{t}Bu.

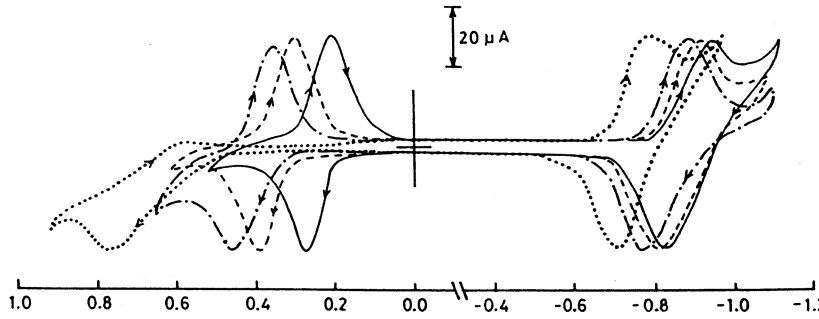

Fig. 3. Cyclic voltammogram of [Pt(HaaiEt)(cat)] (— · —); [Pt(HaaiEt)(cat)] (- - -); [Pt(HaaiEt)(cat)] (—) and [Pt(HaaiEt)(tccat)] (· · ·) in MeCn.

Table 5
Comparison with analogous palladium complexes

Complex	λ_{LLCT} (nm)	$E^{M}_{1/2}$ (V)	$-E^{L}_{1/2}$ (V)
Pd(HaaiEt)(tbcat)	974	0.45	0.46
Pd(HaaiEt)(dtbcat)	1000	0.35	0.50
Pd(MeaaiEt)(tbcat)	944	0.41	0.50
Pd(MeaaiEt)(dtbcat)	982	0.32	0.55
Pt(HaaiEt)(tbcat)	841	0.353	0.868
Pt(HaaiEt)(dtbcat)	925	0.247	0.884
Pt(MeaaiEt)(tbcat)	822	0.338	0.924
Pt(MeaaiEt)(dtbcat)	888	0.214	0.895

backed up by the unusual enhancement of the N=N bond and shortening of the C–O bond in the X-ray crystal structure and supports the charge shifting the catecholate part to the azoimine end.

4. Conclusions

We have isolated platinum(II) complexes of 1-ethyl-2-(arylazo)imidazoles and their dioxolene derivatives. The complexes have been characterised by spectral studies and the structural confirmation of (catecholato){1-ethyl-2-(*p*-tolylazo)imidazole}platinum(II) has been carried out by X-ray crystallography. Solution absorption spectra of catecholato complexes exhibit LLCT spectra in the NIR region. A redox study shows four successive redox responses; two oxidative responses are due to catechol to semiquinone and semiquinone to quinone and two reductive responses are azo reductions. The difference between the first oxidation and first reduction potential is linearly correlated with the energy of the LLCT transition.

5. Supplementary material

For (catecholato){1-ethyl-2-(*p*-tolylazo)imidazole}-platinum(II), Pt(cat)(MeaaiEt), tables of complete bond parameters anisotropic thermal parameters, hydrogen atom positional parameters and other supplementary data are available from the Cambridge Crystallographic Data Centre, 12 Union Road, Cambridge CB2 1EZ, UK, on request, quoting the deposition number 147007.

Acknowledgements

Financial support from the Council of Scientific and Industrial Research, New Delhi is gratefully acknowledged. Our sincere thanks are due to Professor G.N. Mukherjee, Department of Chemistry, Calcutta University for recording some NIR spectra and helpful discussion.

References

[1] S. Goswami, R.N. Mukherjee, A. Chakravorty, Inorg. Chem. 38 (1989) 2989.
[2] B.K. Ghosh, A. Chakravorty, Coord.Chem. Rev. 95 (1989) 239.
[3] B.K. Ghosh, A. Mukhopadhyay, S. Goswami, S. Roy, A. Chakravorty, Inorg. Chem. 23 (1984) 4633.
[4] G.K. Lahiri, S. Goswmi, L.R. Falvello, A. Chakraborty, Inorg. Chem. 26 (1987) 3365.
[5] S. Goswami, A.R. Chakravarty, A. Chakravorty, Inorg. Chem. 22 (1983) 602.
[6] R.A. Krause, K. Krause, Inorg. Chem. 23 (1984) 2195.
[7] M. Shivakumar, K. Pramanik, P. Ghosh, A. Chakravorty, Inorg. Chem. 37 (1998) 5968.
[8] S. Goswami, A.R. Chakravarty, A. Chakravorty, J. Chem. Soc., Chem. Commun. (1982) 1288.
[9] I. Chakraborty, S. Bhattacharya, S. Banerjee, B.K. Dirghangi, A. Chakravorty, J. Chem. Soc., Dalton Trans. (1999) 3747
[10] M. Kakoti, S. Chowdhury, A.K. Deb, S. Goswami, Polyhedron 12 (1993) 783.
[11] P. Majumdar, S. Goswami, S.-M. Peng, Polyhedron 18 (1999) 2543.
[12] A. Saha, A.K. Ghosh, P. Majumdar, K.N. Mitra, S. Mondal, K.K. Rajak, L.R. Falvello, S. Goswami, Organometallics 18 (1999) 3772.
[13] C.K. Pal, S. Chattopadhyay, C. Sinha, D. Bandyopadhyay, A. Chakravorty, Polyhedron 13 (1994) 999.
[14] B.K. Santra, G.A. Thakur, P. Pramanik, G.K. Lahiri, Inorg. Chem. 35 (1996) 3050.
[15] B.K. Santra, P. Munshi, G. Das, P. Bharadwaj, G.K. Lahiri, Polyhedron 18 (1999) 617.
[16] B.K. Santra, G.K. Lahiri, J. Chem. Soc., Dalton Trans. (1997) 1883.

[17] D. Dutta, A. Chakravorty, Inorg. Chem. 22 (1983) 1085.
[18] K. Bag, N.K. De, B.R. De, C. Sinha, Proc. Indian Acad. Sci. (Chem. Sci.) 109 (1997) 159.
[19] T.K. Misra, D. Das, C. Sinha, P. Ghosh, C.K. Pal, Inorg. Chem. 37 (1998) 1672.
[20] T.K. Misra, C. Sinha, Transition Met. Chem. 24 (1999) 467.
[21] T.K. Misra, D. Das, C. Sinha, Polyhedron 16 (1997) 4163.
[22] D. Das, T.K. Misra, C. Sinha, Transition Met. Chem. 23 (1998) 73.
[23] D. Das, C. Sinha, Indian J. Chem. A 37 (1998) 531.
[24] D. Das, C. Sinha, Transition Met. Chem. 23 (1998) 517.
[25] D. Das, A.K. Das, C. Sinha, Talanta 48 (1999) 1013.
[26] D. Das, A.K. Das, C. Sinha, Anal. Lett. 32 (1999) 567.
[27] M. Shivakumar, K. Pramanik, P. Ghosh, A. Chakravorty, J. Chem. Soc., Chem. Commun. (1998) 2104.
[28] P.K. Santra, D. Das, T.K. Misra, R. Roy, C. Sinha, S.-M. Peng, Polyhedron 18 (1999) 1909.
[29] R. Roy, P. Chattopadhyay, C. Sinha, S. Chattopadhyay, Polyhedron 15 (1996) 3361.
[30] M. Kato, C. Kosuge, K. Morii, J.S. Ahn, H. Kitagawa, T. Mitani, M. Matsushita, T. Kato, S. Yano, M. Kimura, Inorg. Chem. 38 (1999) 1638.
[31] J.A. Weinstein, N.N. Zheligovskaya, M.Y. Melnikov, F. Hartl, J. Chem. Soc., Dalton Trans. (1998) 2459.
[32] (a) S.D. Cummings, R. Eisenberg, J. Am. Chem. Soc. 118 (1996) 1949. (b) W. Paw, W.B. Connick, R. Eisenberg, Inorg. Chem. 37 (1998) 3919.
[33] L. Johnson, O.B. Ryan, M. Tilget, J. Am. Chem. Soc. 121 (1999) 1974.
[34] R. Lewis, Scientist 13 (1999) 11.
[35] P.M. Takahara, C.A. Fredrick, S.J. Lippard, J. Am. Chem. Soc. 118 (1996) 12309.
[36] S.J. Lippard, in: I. Bertini, H.B. Gray, S.J. Lippard, J.S. Valentine (Eds.), Bioinorganic Chemistry, University Science Books, Mill Valley, CA, 1994, p. 505.
[37] B. Lippert, Coord. Chem. Rev. 182 (1999) 263.
[38] C.A. McAuliffe, H.L. Sharma, N.D. Tinker, Studies in Inorganic Chemistry II, Chemistry of the Platinum Group Metals. Recent Developments, Elsevier, Amsterdam, 1991, p. 571.
[39] S.S. Kamath, V. Uma, T.S. Srivastava, Inorg. Chim. Acta 166 (1989) 91.
[40] S.E. Livingstone, Synth. React. Inorg. Met. Org. Chem. 1 (1971) 1.
[41] S.R. Hall, H.D. Flack, J.M. Stewart (Eds.), The XTAL 3.2 User's Manual, University of Western Australia, Geneva/Western Australia.
[42] G.M. Sheldrick, Acta Crystallogr, Sect. A 46 (1990) 467.
[43] G.M. Sheldrick, SHELXL97: Program for Crystal Structure Determination, University of Göttingen, Germany.
[44] C.G. Pierpont, R.M. Buchanan, Coord. Chem. Rev. 38 (1981) 45.
[45] G.A. Fox, C.G. Pierpont, J. Chem. Soc., Chem. Commun. (1988) 806.
[46] A. Seal, S. Roy, Acta Crystallogr. Sect. C 40 (1984) 929.
[47] C. Sinha, Ph.D. Thesis, Jadavpur University, India, 1990.
[48] G.K. Routh, S. Pal, D. Das, C. Sinha, A.M.Z. Slawin, J.D. Woollins, in preparation.
[49] D. Das, Ph.D. Thesis, Burdwan University, Burdwan, India, 1998.
[50] S. Pal, D. Das, P. Chattopadhyay, C. Sinha, K. Panneerselvam, T.-H. Lu, Polyhedron 19 (2000) 1263.
[51] H. Engelking, B. Krebs, J. Chem. Soc., Dalton Trans. (1996) 2409.
[52] R. Sahai, D.P. Rillema, Inorg. Chim. Acta 118 (1986) L35.
[53] D.J. Gordon, R.F. Fenske, Inorg. Chem. 21 (1982) 2907.
[54] S. Chattopadhyay, C. Sinha, P. Basu, A. Chakravorty, J. Organomet. Chem. 414 (1991) 421.
[55] D.E. Wheeler, J.H. Rodriguez, J.K. McCusker, J. Phys. Chem. 103 (1999) 4102.
[56] S.B. Kumar, M. Chaudhury, J. Chem. Soc., Dalton Trans. (1991) 2169.
[57] F.A. Cotton, Advanced Inorganic Chemistry, 3rd edn, Wiley Eastern, New Delhi, 1972.